Signature of Cosmic String Wakes in N Body Simulations

Disrael da Cunha, PhD candidate,
supervisor: Robert Brandenberger

McGill University

April 11 - 2018

Content

Current Section

Introduction

T. Kibble, J. Phys. A 9, 1387 (1976); A. Vilenkin and E.P.S. Shellard, Cosmic Strings and other Topological Defects (Cambridge Univ. Press, Cambridge, 1994); T. W. B. Kibble, Phase Transitions In The Early Universe, Acta Phys. Polon. B 13, 723 (1982).

- Cosmic strings are linear topological defects in QFT
- Cosmic strings exist as solutions for models that go beyond the Standard Model of Particle Physics
- One analogy from condensed matter physics is line defects in crystals
- A second analogy is a vortex line in superfluid or superconductor
- Cosmic strings are one dimensional regions of trapped energy with important gravitational effects for cosmology

Introduction

T. Kibble, J. Phys. A 9, 1387 (1976); A. Vilenkin and E.P.S. Shellard, Cosmic Strings and other Topological Defects (Cambridge Univ. Press, Cambridge, 1994); T. W. B. Kibble, Phase Transitions In The Early Universe, Acta Phys. Polon. B 13, 723 (1982); Brandenberger, Robert H. , Topological defects and structure formation (1994)

- If a model of nature admits cosmic string solutions, they will necessarily form in the early universe
- In this case, cosmic strings will persist to the present time as a scaling network

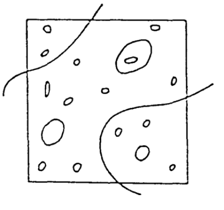

Figure 1: scaling solution for the cosmic string network at an arbitrary time

Introduction

Dvorkin, Hu and Wyman, 2011; A. Vilenkin and E.P.S. Shellard, Cosmic Strings and other Topological Defects (Cambridge Univ. Press, Cambridge, 1994);

- The cosmic string tension μ is given by $G\mu \simeq (\eta/m_{pl})^2$, where η is the energy scale at which they form
- The best robust constraint is $G\mu \approx 1.5 \times 10^{-7}$

Introduction

Brandenberger, Cyr, Iyer (2017); R.B., Y. Cai, W. Xue and X. Zhang (2009); Bramberger, Brandenberger, Jreidini, Quintin (2015)

- Observing cosmic strings can give information about particle physics models
- Constraining μ will rule out classes of particle physics models
- Cosmic strings could produce interesting results for cosmology: FRB, primordial magnetic fields, the origin of supermassive black holes

Introduction

- LSS provides an alternative arena for probing cosmic strings

Current Section

Cosmic string review

A. Vilenkin and E.P.S. Shellard, Cosmic Strings and other Topological Defects (Cambridge Univ. Press, Cambridge, 1994);

- Simple abelian Higgs model with scalar field potential

$$V = \lambda(\Phi\Phi^* - \frac{\eta^2}{2})^2$$

- At very high temperatures $\Phi \approx 0$.
- At temperatures below η the scalar field acquires a non-zero v.e.v. and a symmetry breaking occurs
- The potential is minimized for $|\Phi|^2 = \frac{\eta^2}{2}$
  $\therefore \Phi = (\frac{\eta}{\sqrt{2}})e^{i\theta}$ is the minimum energy manifold

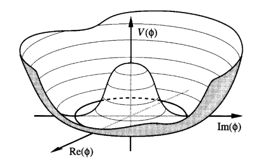

Figure 2: Mexican Hat Potential (Vilenkin 1994)

Cosmic string review

H. B. Nielsen e P. Olesen, Nucl. Phys. B61, 45 (1973); A. Vilenkin, Phys. Rev. D 23, 852 (1981)

- The phases of the scalar field in different Hubble volumes must be uncorrelated by causality
- Therefore there is a probability $\approx O(1)$ that given a circle with the Hubble radius, the phase of the field will change by a non-zero multiple of 2π
- There exist a point on every surface that has this circle as boundary such that the field is zero
- The collection of these points forms a tube with trapped energy: the cosmic string
- The linear mass density of the string satisfy $G\mu = (\frac{\eta}{m_{pl}})^2$

Cosmic string network

A. Vilenkin and E.P.S. Shellard, Cosmic Strings and other Topological Defects (Cambridge Univ. Press, Cambridge, 1994);

- After they form, cosmic strings produces a scaling network
- The main reason is that cosmic strings exchange ends when they collide

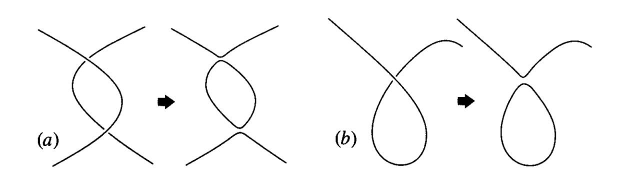

- This causes loop production
- Loops oscillate and release energy through a radiation channel

Cosmic string network

A. Vilenkin and E.P.S. Shellard, Cosmic Strings and other Topological Defects (Cambridge Univ. Press, Cambridge, 1994);

- The cosmic string network is characterized by a correlation length $\xi(t)$
- If $\xi(t)/t > 1$ then ξ freezes and $\xi(t)/t$ decreases
- If $\xi(t)/t < 1$ then many loops will form and radiate energy away from the strings, increasing $\xi(t)/t$
- Therefore $\xi(t) \approx t$ is a stable solution

Current Section

Wake formation

- Conical space: deficit angle $\alpha = 8\pi G\mu$
- Introduces velocity perturbations $\delta v = 4\pi\gamma_s v_s G\mu$

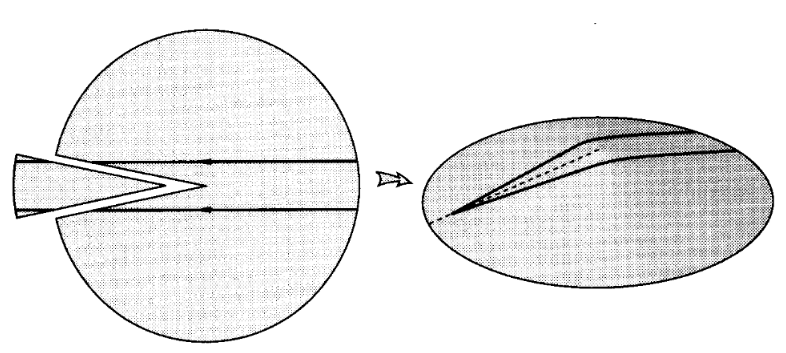

Figure 3: Effect on the LSS (Vilenkin 1994)

Wake formation

A. Stebbins, S. Veeraraghavan, Rm H. Brandenberger, J. Silk e N. Turok, Cosmic String Wakes, Astrophys. J. 233, 1 (1987); A. Vilenkin and E.P.S. Shellard, Cosmic Strings and other Topological Defects (Cambridge Univ. Press, Cambridge, 1994)

- The deficit angle create a wedge-like structure called wake

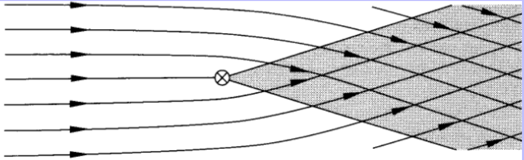

Figure 4: Effect on the LSS (Vilenkin 1994)

- The wake has the following dimensions

$$V \approx t_i \times t_i v_s \gamma_s \times 4\pi G\mu t_i v_s \gamma_s$$

- The wake produces a non linear density fluctuation at arbitrarily early times

Wake evolution I

J. Silk and A. Vilenkin, Phys. Rev. Lett. 53, 1700 (1984)

- Physical distance to the wake

$$h(q,t) = a(t)[q - \psi(q,t)]$$

- Initial condition

$$\psi(t_i) = 0 \quad , \quad \dot{\psi}(t_i) = 4\pi\gamma_s v_s G\mu$$

- Zel'dovich approximation

$$\ddot{h} = -\frac{\partial \Phi}{\partial h} \quad , \quad \frac{\partial^2 \Phi}{\partial h^2} = 4\pi G[\rho + \sigma\delta(h)]$$

$$\sigma(t) = 4\pi G\mu t_i v_s \gamma_s \left(\frac{t}{t_i}\right)^{\frac{2}{3}} \rho(t)$$

Wake evolution II

J. Silk and A. Vilenkin, Phys. Rev. Lett. 53, 1700 (1984)

- Linearized equation

$$\ddot{\psi} + \frac{4}{3t}\dot{\psi} - \frac{2}{3t^2}\psi = 0$$

- Growing mode solution

$$\psi(t) = \frac{12\pi}{5} G\mu v_s \gamma_s t_i \left(\frac{t}{t_i}\right)^{\frac{2}{3}}$$

- Turn around point ($\dot{h} = 0$)

$$q_{ta} = \frac{24\pi}{5} G\mu v_s \gamma_s t_0 \frac{\sqrt{1+z_i}}{(1+z)}$$

Wake evolution III

J. Silk and A. Vilenkin, Phys. Rev. Lett. 53, 1700 (1984)

- Double density

$$\psi(q_{ta}, t) = \frac{1}{2} q_{ta}$$

- Wake thickness

$$\psi_3 = \frac{24\pi}{5} G\mu v_s \gamma_s t_0 \frac{\sqrt{1+z_i}}{(1+z)}$$

- Thickness is higher for wakes produced at early times
- The wake accrete matter and grows in thickness proportionally to the scale factor

Current Section

Studying wake disruption

- LCDM fluctuations grows in 3 dimensions while the wake only grows in 1 dimension

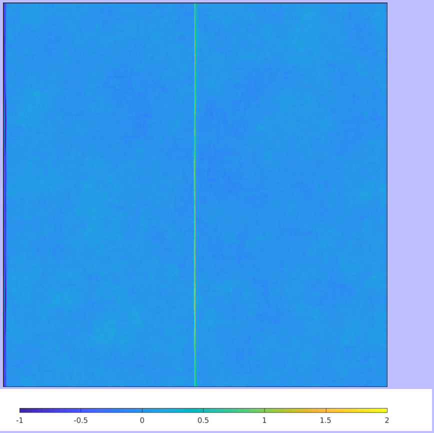

Figure 5: a $G\mu = 4 \times 10^{-6}$ wake , $z = 31$

Studying wake disruption

- LCDM fluctuations grows in 3 dimensions while the wake only grows in 1 dimension

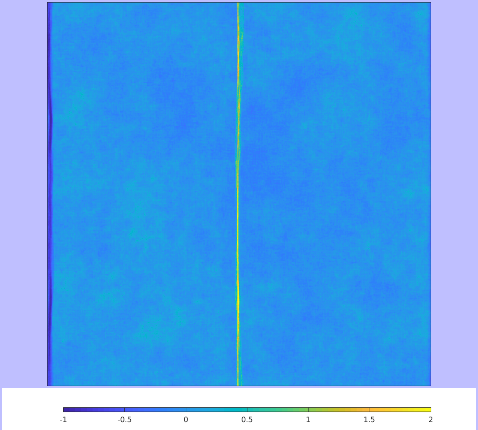

Figure 5: a $G\mu = 4 \times 10^{-6}$ wake , $z = 15$

Studying wake disruption

- LCDM fluctuations grows in 3 dimensions while the wake only grows in 1 dimension

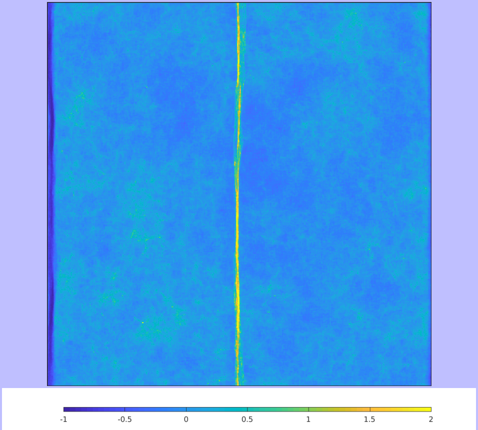

Figure 5: a $G\mu = 4 \times 10^{-6}$ wake , $z = 10$

Studying wake disruption

- LCDM fluctuations grows in 3 dimensions while the wake only grows in 1 dimension

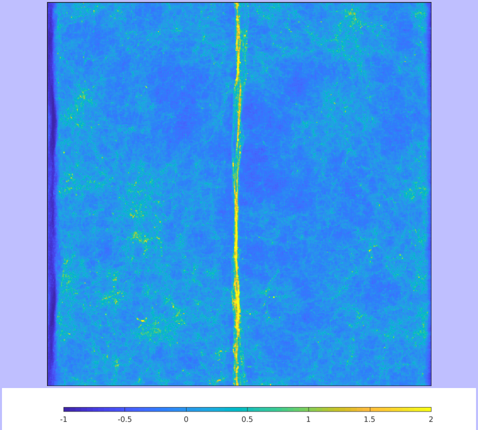

Figure 5: a $G\mu = 4 \times 10^{-6}$ wake , $z = 7$

Studying wake disruption

- LCDM fluctuations grows in 3 dimensions while the wake only grows in 1 dimension

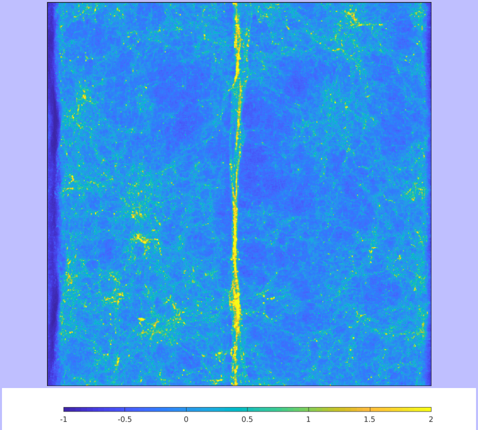

Figure 5: a $G\mu = 4 \times 10^{-6}$ wake , $z = 5$

Studying wake disruption

- LCDM fluctuations grows in 3 dimensions while the wake only grows in 1 dimension

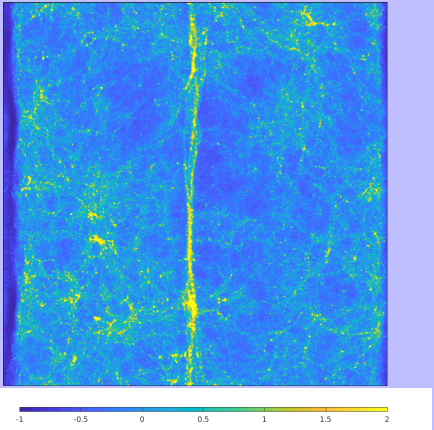

Figure 5: a $G\mu = 4 \times 10^{-6}$ wake , $z = 4$

Studying wake disruption

- LCDM fluctuations grows in 3 dimensions while the wake only grows in 1 dimension

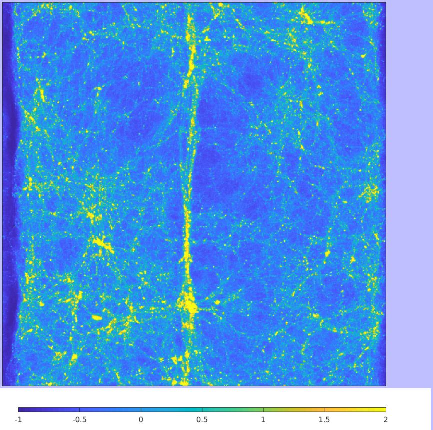

Figure 5: a $G\mu = 4 \times 10^{-6}$ wake , $z = 3$

Studying wake disruption

- LCDM fluctuations grows in 3 dimensions while the wake only grows in 1 dimension

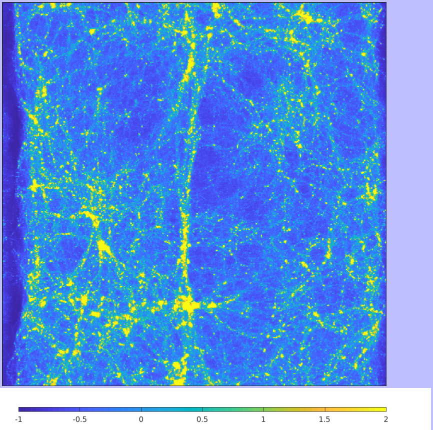

Figure 5: a $G\mu = 4 \times 10^{-6}$ wake , $z = 2$

Studying wake disruption

- LCDM fluctuations grows in 3 dimensions while the wake only grows in 1 dimension

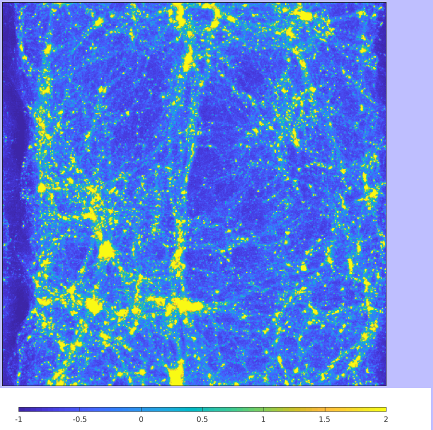

Figure 5: a $G\mu = 4 \times 10^{-6}$ wake , $z = 1$

Studying wake disruption

- LCDM fluctuations grows in 3 dimensions while the wake only grows in 1 dimension

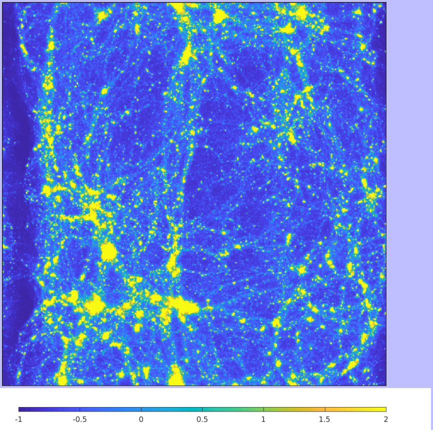

Figure 5: a $G\mu = 4 \times 10^{-6}$ wake , $z = 0.5$

Studying wake disruption

- LCDM fluctuations grows in 3 dimensions while the wake only grows in 1 dimension
- One way to study the local wake disruption is to consider a small box with the wake thickness dimension

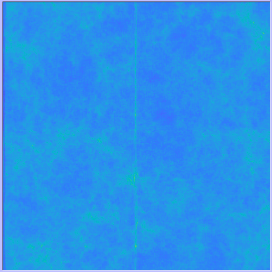

Studying wake disruption

- LCDM fluctuations grows in 3 dimensions while the wake only grows in 1 dimension
- One way to study the local wake disruption is to consider a small box with the wake thickness dimension

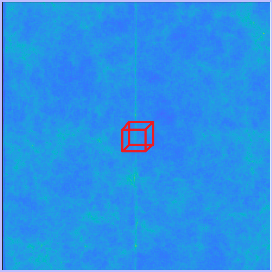

Local Delta condition

Brandenberger, Hernández and DC, arXiv 1508.02317

- If the variance Δ^2 of the density contrast is approximately one, then the wake is locally disrupted:

$$\Delta^2(\psi_3(z), z) \approx 1$$

- The tension of cosmic string wake that will be locally disrupted at a given redshift is shown below

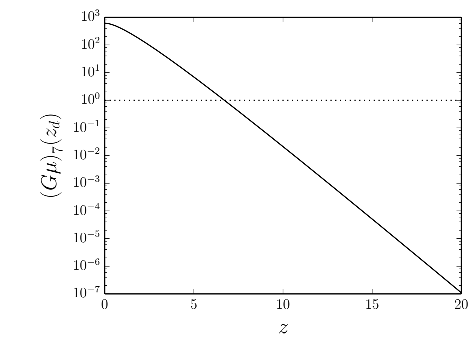

Global sigma condition

Brandenberger, Hernández and DC, arXiv 1508.02317

- The previous criteria missed the global volume of the wake, so a natural extension would be to consider a box with the dimensions of the whole wake.

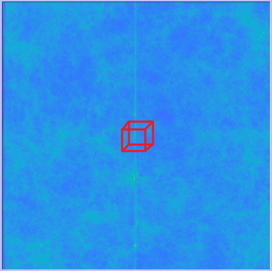

Global sigma condition

Brandenberger, Hernández and DC, arXiv 1508.02317

- The previous criteria missed the global volume of the wake, so a natural extension would be to consider a box with the dimensions of the whole wake.

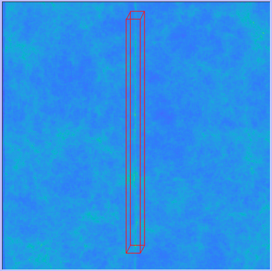

Global sigma condition

Brandenberger, Hernández and DC, arXiv 1508.02317

- The resulting standard deviation in the wake region is :

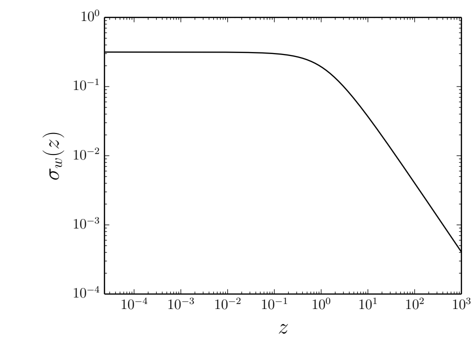

Current Section

Setup of the simulation

J. Harnois-Deraps, U. L. Pen, I. T. Iliev, H. Merz,J. D. Emberson and V. Desjacques, High Performance P3M N-body code: CUBEP3M, Mon. Not. Roy. Astron. Soc. 436, 540 (2013)

- CUBEP3M N-body simulation code
- Initial conditions of the particle distribution were modified

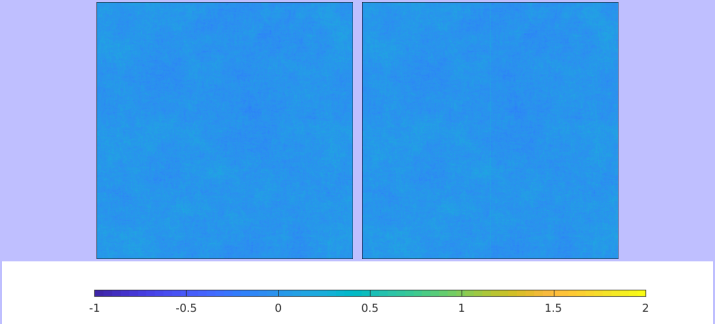

Figure 5: with no wake (left), a wake $G\mu = 8 \times 10^{-7}$ (right),$z = 31$

Setup of the simulation

J. Harnois-Deraps, U. L. Pen, I. T. Iliev, H. Merz, J. D. Emberson and V. Desjacques, High Performance P3M N-body code: CUBEP3M, Mon. Not. Roy. Astron. Soc. 436, 540 (2013)

- CUBEP3M N-body simulation code
- Initial conditions of the particle distribution were modified

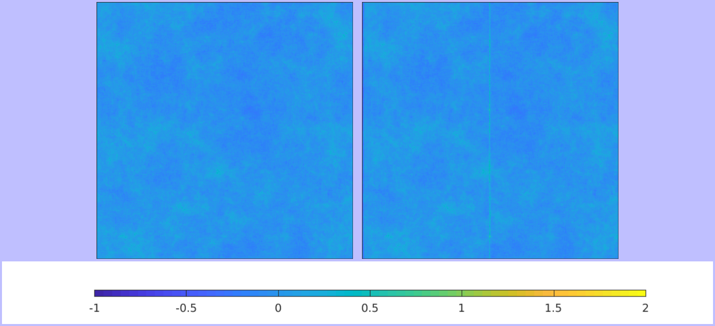

Figure 5: with no wake (left), a wake $G\mu = 8 \times 10^{-7}$ (right), $z = 15$

Setup of the simulation

J. Harnois-Deraps, U. L. Pen, I. T. Iliev, H. Merz,J. D. Emberson and V. Desjacques, High Performance P3M N-body code: CUBEP3M, Mon. Not. Roy. Astron. Soc. 436, 540 (2013)

- CUBEP3M N-body simulation code
- Initial conditions of the particle distribution were modified

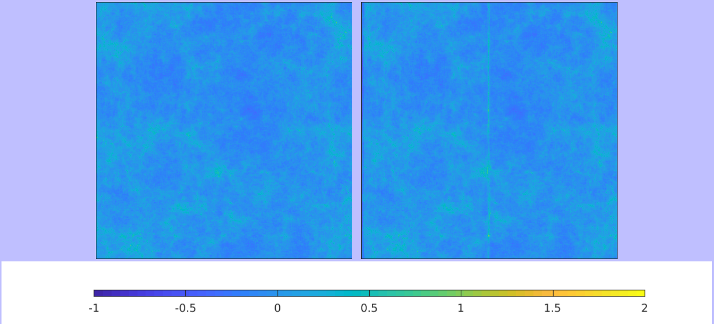

Figure 5: with no wake (left), a wake $G\mu = 8 \times 10^{-7}$ (right),$z = 10$

Setup of the simulation

J. Harnois-Deraps, U. L. Pen, I. T. Iliev, H. Merz,J. D. Emberson and V. Desjacques, High Performance P3M N-body code: CUBEP3M, Mon. Not. Roy. Astron. Soc. 436, 540 (2013)

- CUBEP3M N-body simulation code
- Initial conditions of the particle distribution were modified

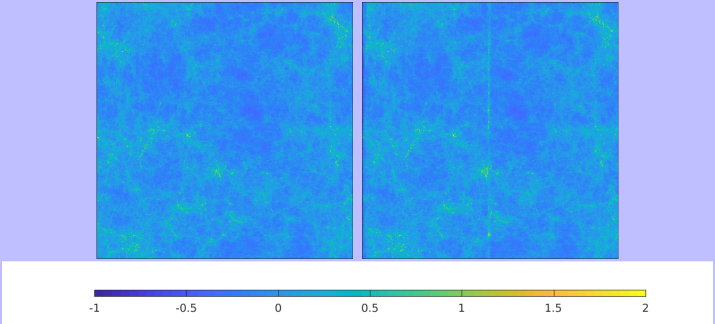

Figure 5: with no wake (left), a wake $G\mu = 8 \times 10^{-7}$ (right),$z = 7$

Setup of the simulation

J. Harnois-Deraps, U. L. Pen, I. T. Iliev, H. Merz,J. D. Emberson and V. Desjacques, High Performance P3M N-body code: CUBEP3M, Mon. Not. Roy. Astron. Soc. 436, 540 (2013)

- CUBEP3M N-body simulation code
- Initial conditions of the particle distribution were modified

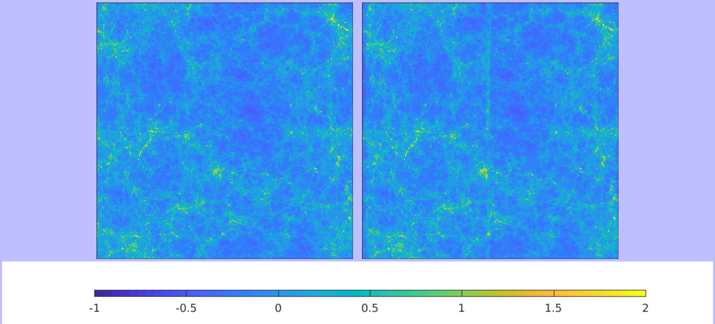

Figure 5: with no wake (left), a wake $G\mu = 8 \times 10^{-7}$ (right),$z = 5$

Setup of the simulation

J. Harnois-Deraps, U. L. Pen, I. T. Iliev, H. Merz,J. D. Emberson and V. Desjacques, High Performance P3M N-body code: CUBEP3M, Mon. Not. Roy. Astron. Soc. 436, 540 (2013)

- CUBEP3M N-body simulation code
- Initial conditions of the particle distribution were modified

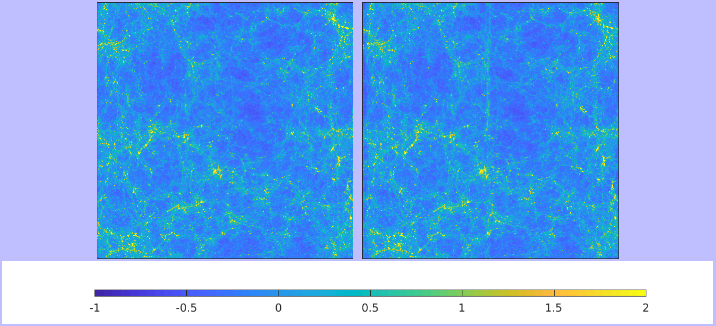

Figure 5: with no wake (left), a wake $G\mu = 8 \times 10^{-7}$ (right),$z = 4$

Setup of the simulation

J. Harnois-Deraps, U. L. Pen, I. T. Iliev, H. Merz,J. D. Emberson and V. Desjacques, High Performance P3M N-body code: CUBEP3M, Mon. Not. Roy. Astron. Soc. 436, 540 (2013)

- CUBEP3M N-body simulation code
- Initial conditions of the particle distribution were modified

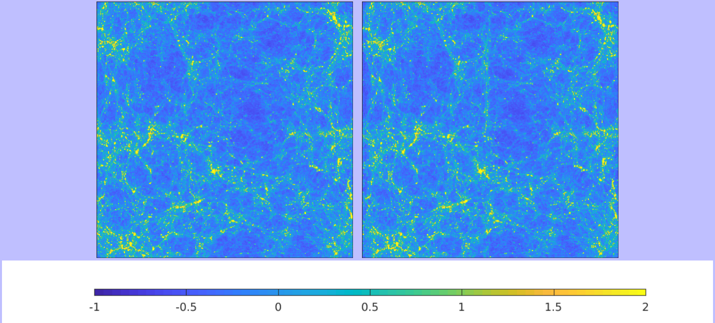

Figure 5: with no wake (left), a wake $G\mu = 8 \times 10^{-7}$ (right),$z = 3$

Setup of the simulation

J. Harnois-Deraps, U. L. Pen, I. T. Iliev, H. Merz,J. D. Emberson and V. Desjacques, High Performance P3M N-body code: CUBEP3M, Mon. Not. Roy. Astron. Soc. 436, 540 (2013)

- CUBEP3M N-body simulation code
- Initial conditions of the particle distribution were modified

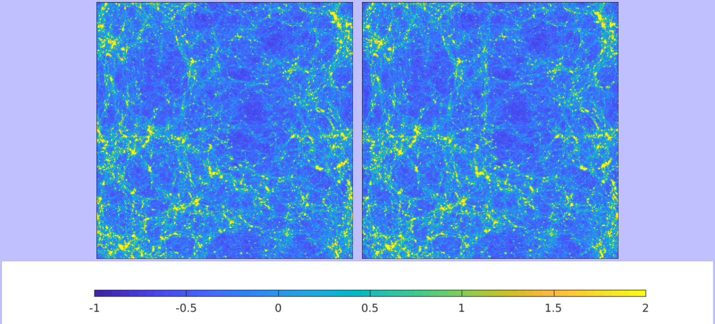

Figure 5: with no wake (left), a wake $G\mu = 8 \times 10^{-7}$ (right),$z = 2$

Setup of the simulation

J. Harnois-Deraps, U. L. Pen, I. T. Iliev, H. Merz,J. D. Emberson and V. Desjacques, High Performance P3M N-body code: CUBEP3M, Mon. Not. Roy. Astron. Soc. 436, 540 (2013)

- CUBEP3M N-body simulation code
- Initial conditions of the particle distribution were modified

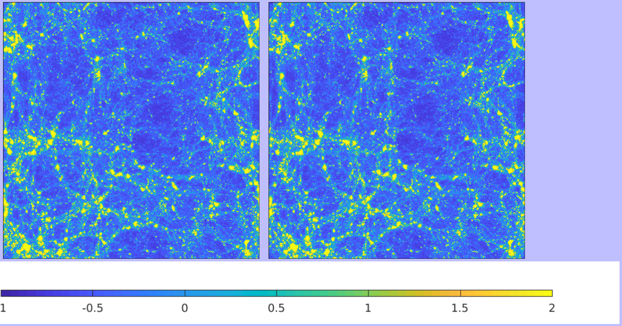

Figure 5: with no wake (left), a wake $G\mu = 8 \times 10^{-7}$ (right),$z = 1$

Setup of the simulation

J. Harnois-Deraps, U. L. Pen, I. T. Iliev, H. Merz,J. D. Emberson and V. Desjacques, High Performance P3M N-body code: CUBEP3M, Mon. Not. Roy. Astron. Soc. 436, 540 (2013)

- CUBEP3M N-body simulation code
- Initial conditions of the particle distribution were modified

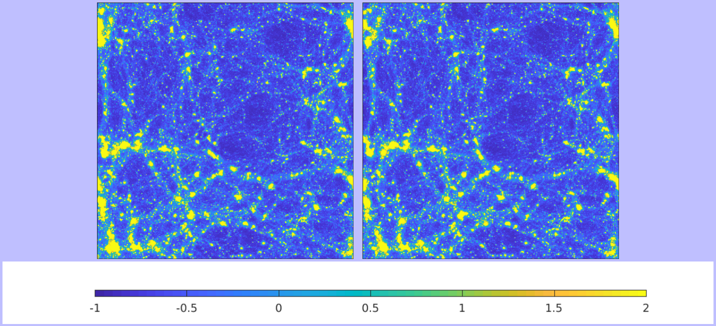

Figure 5: with no wake (left), a wake $G\mu = 8 \times 10^{-7}$ (right),$z = 0$

Global wake overdensity

- Computation of the density inside slices
- One dimensional projection result

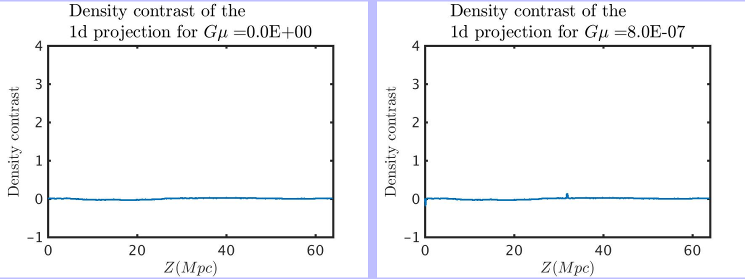

Figure 6: with no wake (left), a wake $G\mu = 8 \times 10^{-7}$ (right), $z = 31$

Global wake overdensity

- Computation of the density inside slices
- One dimensional projection result

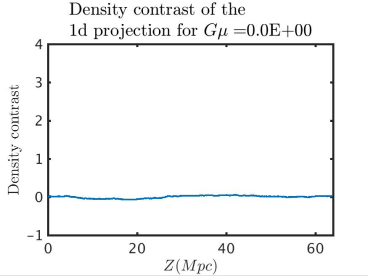

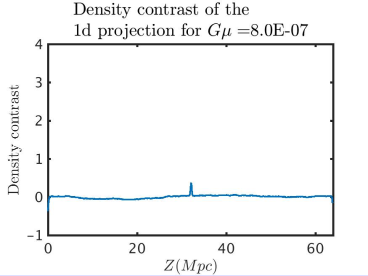

Figure 6: with no wake (left), a wake $G\mu = 8 \times 10^{-7}$ (right), $z = 15$

Global wake overdensity

- Computation of the density inside slices
- One dimensional projection result

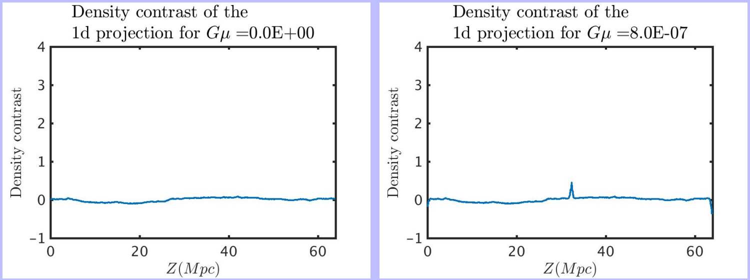

Figure 6: with no wake (left), a wake $G\mu = 8 \times 10^{-7}$ (right), $z = 10$

Global wake overdensity

- Computation of the density inside slices
- One dimensional projection result

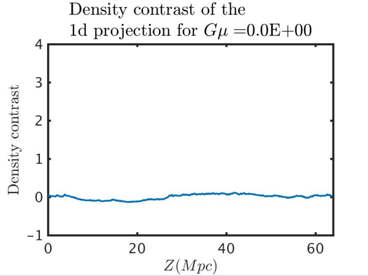

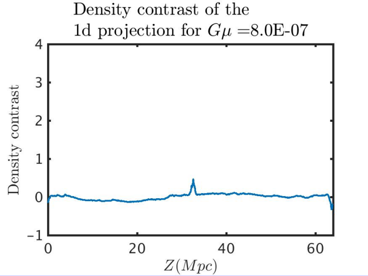

Figure 6: with no wake (left), a wake $G\mu = 8 \times 10^{-7}$ (right), $z = 7$

Global wake overdensity

- Computation of the density inside slices
- One dimensional projection result

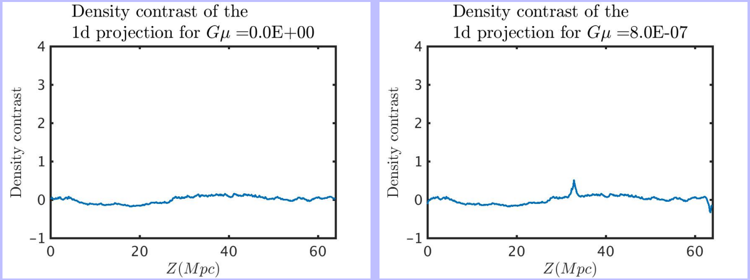

Figure 6: with no wake (left), a wake $G\mu = 8 \times 10^{-7}$ (right), $z = 5$

Global wake overdensity

- Computation of the density inside slices
- One dimensional projection result

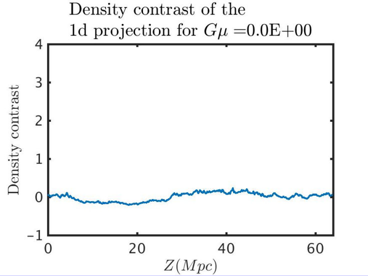

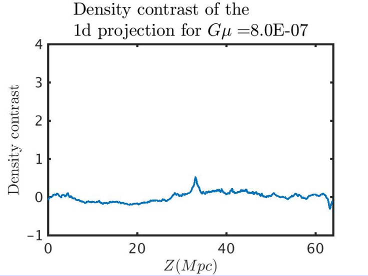

Figure 6: with no wake (left), a wake $G\mu = 8 \times 10^{-7}$ (right), $z = 4$

Global wake overdensity

- Computation of the density inside slices
- One dimensional projection result

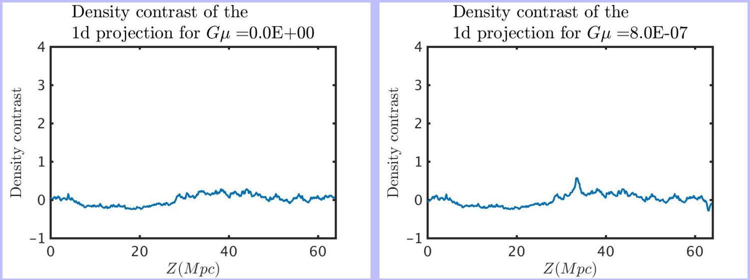

Figure 6: with no wake (left), a wake $G\mu = 8 \times 10^{-7}$ (right), $z = 3$

Global wake overdensity

- Computation of the density inside slices
- One dimensional projection result

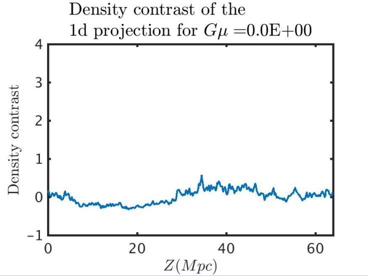

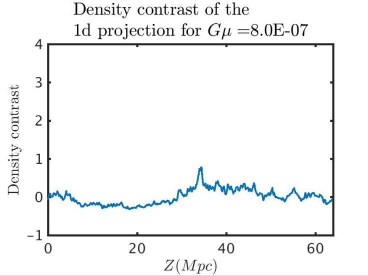

Figure 6: with no wake (left), a wake $G\mu = 8 \times 10^{-7}$ (right), $z = 2$

Global wake overdensity

- Computation of the density inside slices
- One dimensional projection result

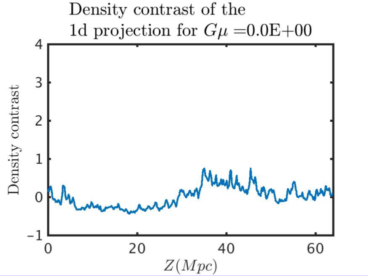

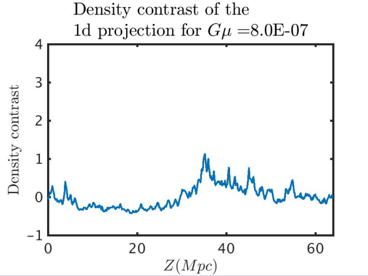

Figure 6: with no wake (left), a wake $G\mu = 8 \times 10^{-7}$ (right), $z = 1$

Global wake overdensity

- Computation of the density inside slices
- One dimensional projection result

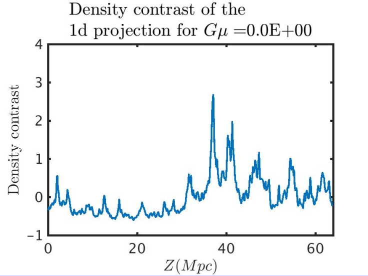

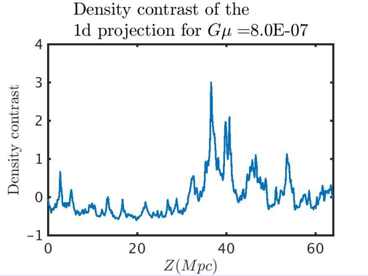

Figure 6: with no wake (left), a wake $G\mu = 8 \times 10^{-7}$ (right), $z = 0$

Dropping the wake orientation prior

- The previous analysis is repeated for many different orientations
- If the wake signal is clear on the one dimensional projections it will correspond to the peak of the density contrast

Spherical maps

- A spherical map is generated in which each point on the sphere corresponds to a pair of angles and the color corresponds to the peak of the density of the associated 1D projection:

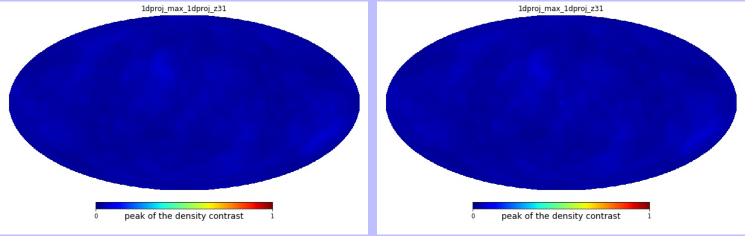

Figure 7: with no wake (left) and with a wake $G\mu = 8 \times 10^{-7}$ (right), $z = 31$

Spherical maps

- A spherical map is generated in which each point on the sphere corresponds to a pair of angles and the color corresponds to the peak of the density of the associated 1D projection:

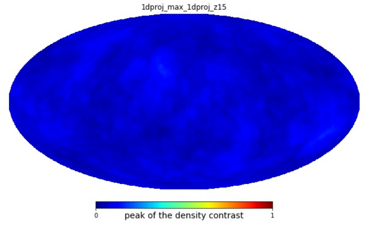

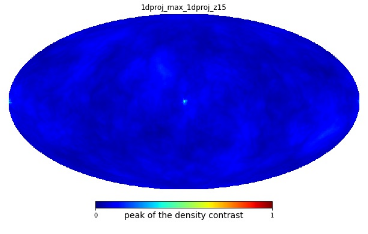

Figure 7: with no wake (left) and with a wake $G\mu = 8 \times 10^{-7}$ (right), $z = 15$

Spherical maps

- A spherical map is generated in which each point on the sphere corresponds to a pair of angles and the color corresponds to the peak of the density of the associated 1D projection:

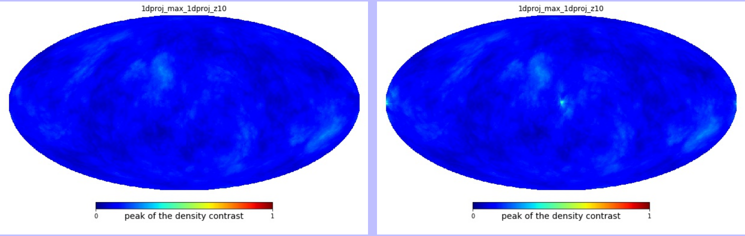

Figure 7: with no wake (left) and with a wake $G\mu = 8 \times 10^{-7}$ (right), $z = 10$

Spherical maps

- A spherical map is generated in which each point on the sphere corresponds to a pair of angles and the color corresponds to the peak of the density of the associated 1D projection:

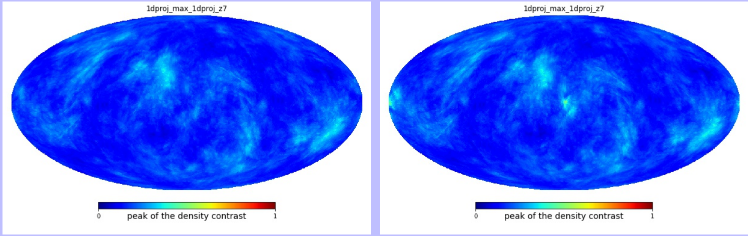

Figure 7: with no wake (left) and with a wake $G\mu = 8 \times 10^{-7}$ (right), $z = 7$

Beyond peak detection

- Large scale density fluctuations can contaminate the wake characterization if it is based only in peaks :

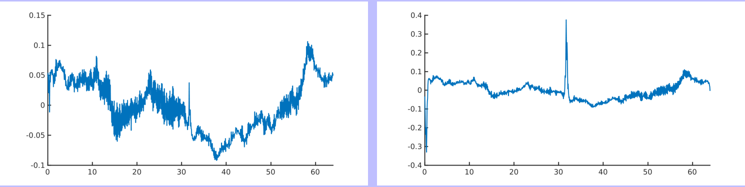

Figure 8: $G\mu = 1 \times 10^{-7}$ wake (left) and with a $G\mu = 8 \times 10^{-7}$ wake (right), $z = 10$

Beyond peak detection

- A good way to focus only on the relevant scale of interest is to analyze the data using the wavelet multiresolution decomposition
- This technique provides the localized features on different scales.

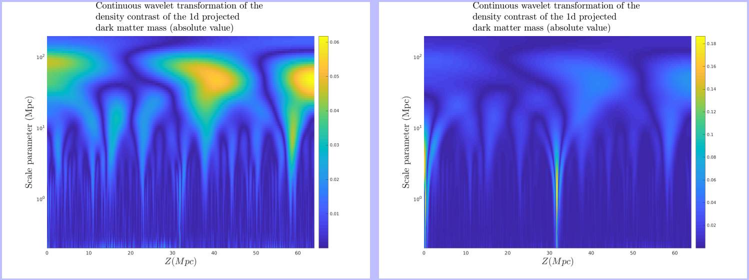

Figure 9: $G\mu = 1 \times 10^{-7}$ wake (left) and with a $G\mu = 8 \times 10^{-7}$ wake (right), $z = 10$

Beyond peak detection

- A good way to focus only on the relevant scale of interest is to analyze the data using the wavelet multiresolution decomposition
- This technique provides the localized features on different scales.

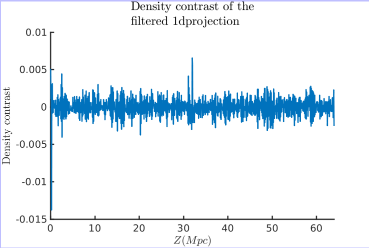

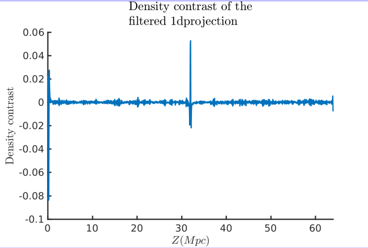

Figure 9: $G\mu = 1 \times 10^{-7}$ wake (left) and with a $G\mu = 8 \times 10^{-7}$ wake (right), $z = 10$

Beyond peak detection

- A good way to focus only on the relevant scale of interest is to analyze the data using the wavelet multiresolution decomposition
- This technique provides the localized features on different scales.

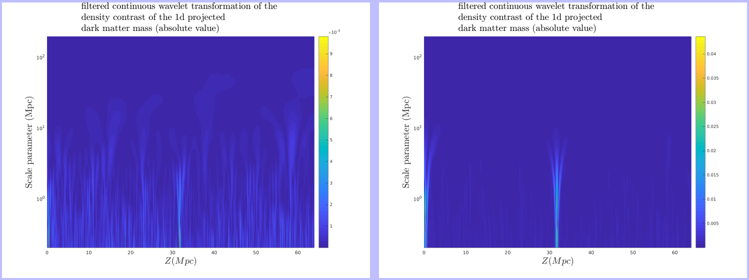

Figure 9: $G\mu = 1 \times 10^{-7}$ wake (left) and with a $G\mu = 8 \times 10^{-7}$ wake (right), $z = 10$

Filtered spherical maps

- With no filtering, the spherical map with a $G\mu = 1 \ \times 10^{7}$ is indistinguishable from the map without a wake

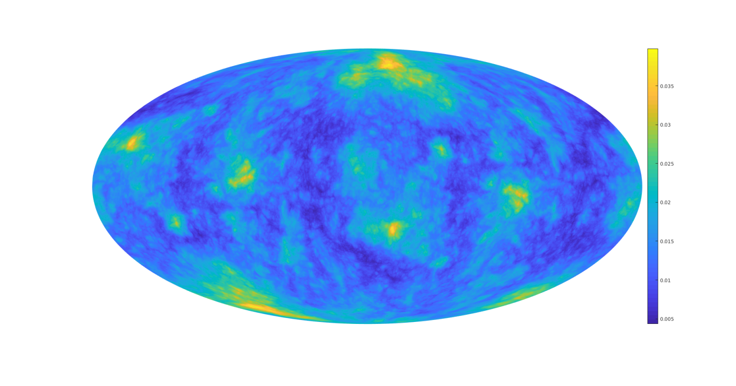

Figure 10: no wake , $z = 10$

Filtered spherical maps

- With no filtering, the spherical map with a $G\mu = 1 \ \times 10^7$ is indistinguishable from the map without a wake

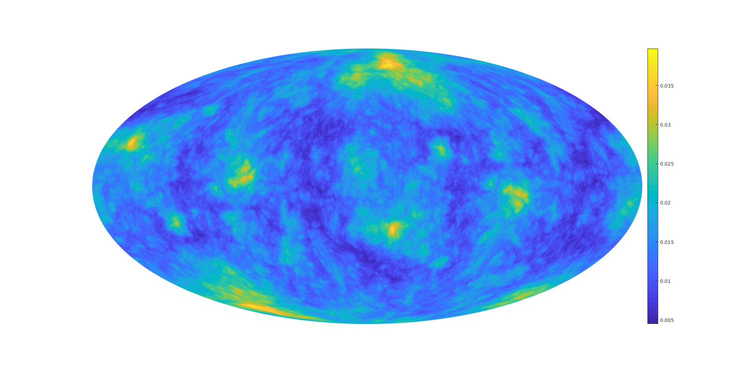

Figure 10: a $G\mu = 1 \times 10^{-7}$ wake , $z = 10$

Filtered spherical maps

- With no filtering, the spherical map with a $G\mu = 1 \times 10^7$ is indistinguishable from the map without a wake

Figure 10: no wake , $z = 10$

Filtered spherical maps

- With no filtering, the spherical map with a $G\mu = 1 \ \times 10^7$ is indistinguishable from the map without a wake

Figure 10: a $G\mu = 8 \times 10^{-7}$ wake , $z = 10$

Filtered spherical maps

- The wavelet analysis is now performed in each direction and the wake is identifiable

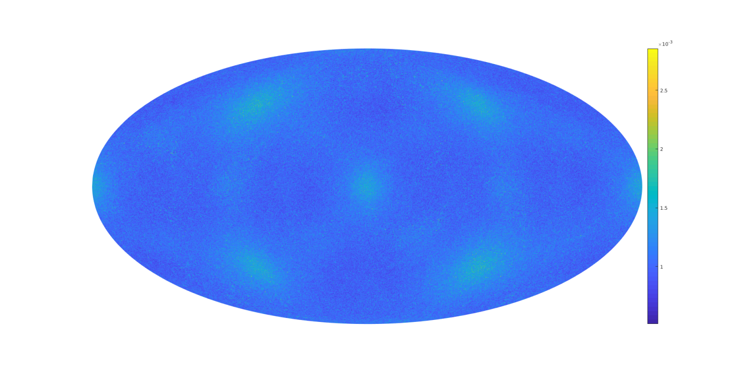

Figure 10: no wake, $z = 10$

Filtered spherical maps

- The wavelet analysis is now performed in each direction and the wake is identifiable

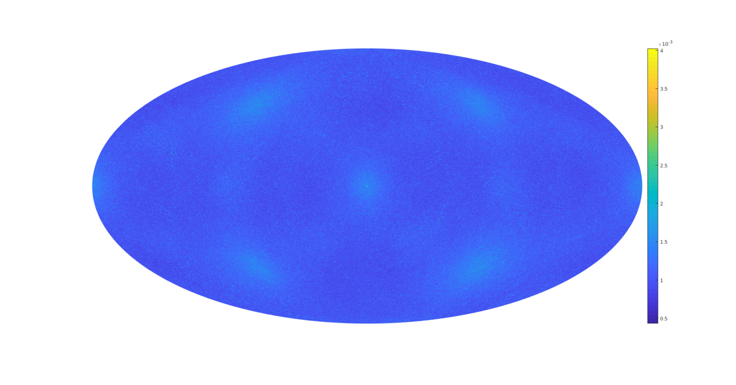

Figure 10: a $G\mu = 8 \times 10^{-7}$ wake, $z = 10$

Filtered spherical maps

- The wavelet analysis is now performed in each direction and the wake is identifiable

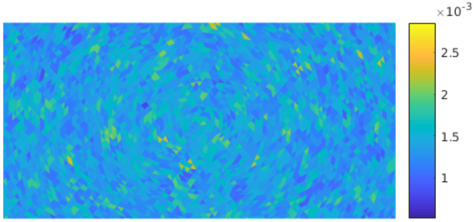

Figure 10: no wake , $z = 10$

Filtered spherical maps

- The wavelet analysis is now performed in each direction and the wake is identifiable

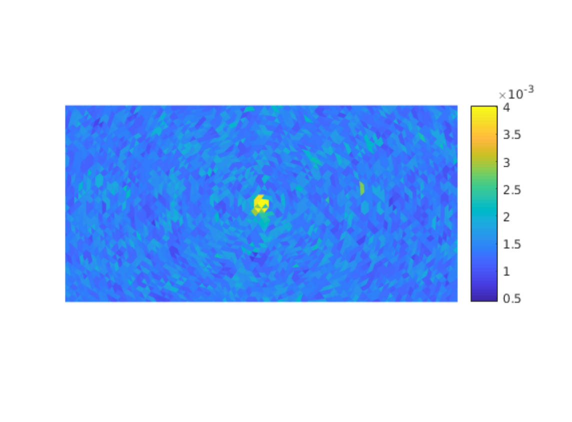

Figure 10: a $G\mu = 8 \times 10^{-7}$ wake, $z = 10$

Sample analysis

DC and Harnois-Deraps, Brandenberger, Amara and Refregier, arXiv 1804.00083

- Repeating the 1d wavelet analysis for different simulations leads to the following result

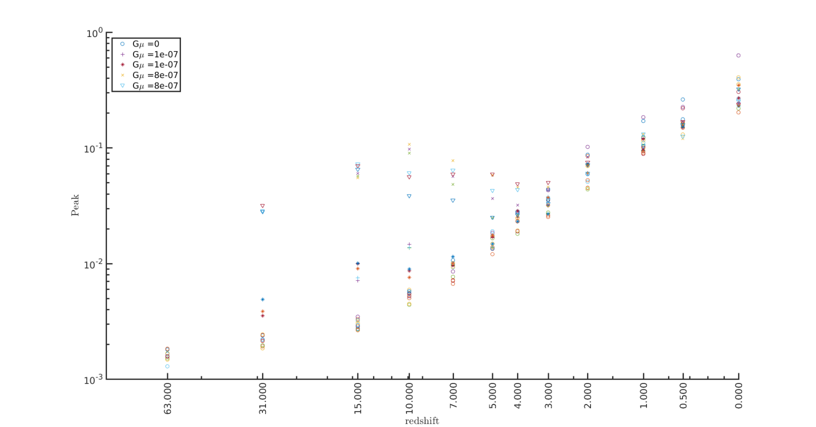

Sample analysis

DC and Harnois-Deraps, Brandenberger, Amara and Refregier, arXiv 1804.00083

- With many samples we can obtain the signal to noise analysis

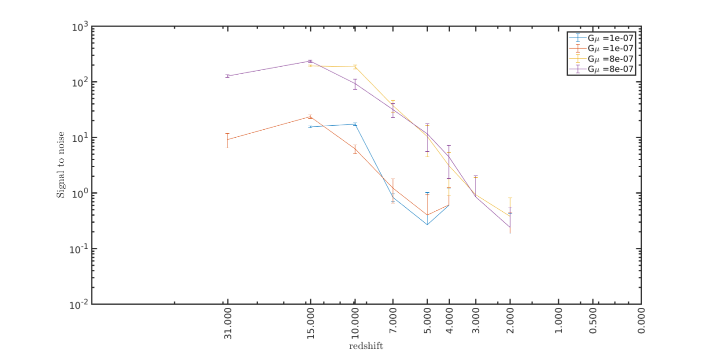

Current Section

Summary

- Wakes of cosmic string can lead to distinguishable signals on the large scale structure
- Wavelet analysis of the dark matter product of N-Body simulations can locate $G\mu = 1 \times 10^{-7}$ wakes at $z = 10$

Future work

- Obtain the sample analysis for the spherical maps
- Explore other statistical methods: Spherical wavelets, AI techniques
- Connect with observations: populate halos with galaxies, analyze 21cm and optical experiments;
- Increase the resolution of the simulation to better resolve the wake
- Consider the network of wakes
- Study non-straight wakes

Thank you